Title

Ni/Photoredox-Catalyzed Enantioselective Cross-Electrophile Coupling of Styrene Oxides with Aryl Iodides

Journal

Journal of the American Chemical Society, 143(38)

ISSN

0002-7863

Authors

Lau, Sii Hong
Borden, Meredith A
Steiman, Talia J
et al.

Publication Date

2021-09-29

DOI

10.1021/jacs.1c08105

Peer reviewed

Published in final edited form as:

J Am Chem Soc. 2021 September 29; 143(38): 15873–15881. doi:10.1021/jacs.1c08105.

Ni/Photoredox-Catalyzed Enantioselective Cross-Electrophile Coupling of Styrene Oxides with Aryl Iodides

Sii Hong Lau[†], **Meredith A. Borden**[†], **Talia J. Steiman**[‡], **Lucy S. Wang**[‡], **Marvin Parasram**, **Abigail G. Doyle**

Department of Chemistry, Princeton University, Princeton, New Jersey 08544, United States

Department of Chemistry & Biochemistry, University of California, Los Angeles, California 90095, United States

Abstract

A Ni/photoredox-catalyzed enantioselective reductive coupling of styrene oxides and aryl iodides is reported. This reaction affords access to enantioenriched 2,2-diarylalcohols from racemic epoxides via a stereoconvergent mechanism. Multivariate linear regression (MVLR) analysis with 29 bioxazoline (BiOx) and biimidazoline (BiIm) ligands revealed that enantioselectivity correlates with electronic properties of the ligands, with more electron-donating ligands affording higher ee's. Experimental and computational mechanistic studies were conducted, lending support to the hypothesis that reductive elimination is enantiodetermining and the electronic character of the ligands influences the enantioselectivity by altering the position of the transition state structure along the reaction coordinate. This study demonstrates the benefits of utilizing statistical modeling as a platform for mechanistic understanding and provides new insight into an emerging class of chiral ligands for stereoconvergent Ni and Ni/photoredox cross-coupling.

Graphical Abstract

Corresponding Author: Abigail G. Doyle – Department of Chemistry and Biochemistry, University of California, Los Angeles, California, 90095, United States; agdoyle@chem.ucla.edu.
Sii Hong Lau – Department of Chemistry, Princeton University, Princeton, New Jersey 08544, United States;
Meredith A. Borden – Department of Chemistry, Princeton University, Princeton, New Jersey 08544, United States;
Talia J. Steiman – Department of Chemistry, Princeton University, Princeton, New Jersey 08544, United States
Lucy S. Wang – Department of Chemistry, Princeton University, Princeton, New Jersey 08544, United States
Marvin Parasram – Department of Chemistry, Princeton University, Princeton, New Jersey 08544, United States;
[†]These authors contributed equally.
[‡]These authors contributed equally.

Supporting Information
The Supporting Information is available free of charge on the ACS Publications website.
Experimental details, optimization studies and characterization data (PDF)
R Source Code (TXT)

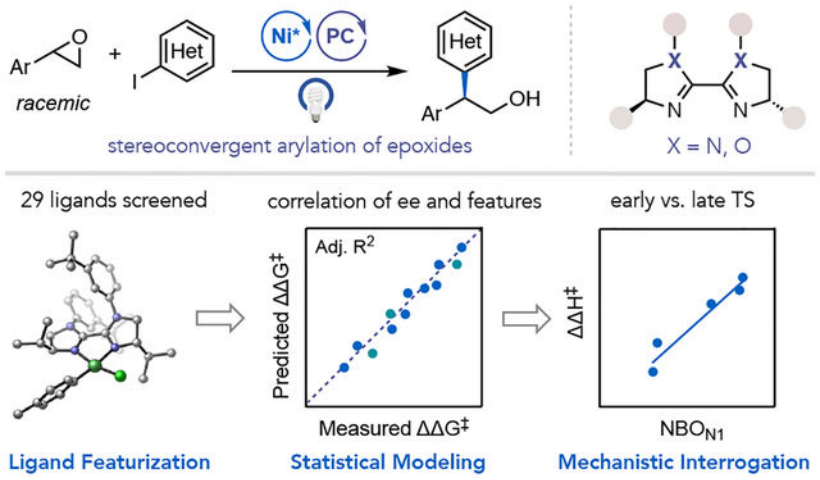

INTRODUCTION

Epoxides are among the most versatile building blocks in organic synthesis due to their availability from olefins and proclivity toward ring-opening by various nucleophiles.[1] Moreover, advances in asymmetric catalytic epoxidation have made enantiomerically-enriched epoxides useful chiral precursors for stereospecific ring-opening.[2] Alternatively, chiral catalyst-controlled asymmetric ring-opening of epoxides represents an attractive method for enantioselective synthesis (Figure 1A).[3] Significant and enabling advances in this area have been realized predominantly with soft or heteroatom-centered nucleophiles, such as azide, water, and cyanide.[4] While asymmetric catalytic C–C bond formation can also be achieved using organolithium and organomagnesium reagents, these methods suffer from harsh conditions and poor functional group tolerance.[5] Furthermore, reactions with chiral epoxide substrates proceed by kinetic resolution owing to a stereospecific ring-opening step. For both practical and fundamental reasons, development of chiral catalyst-controlled stereoconvergent C–C bond-forming reactions of racemic epoxides would be of high value.

Transition-metal catalyzed cross-coupling offers a mild and versatile approach to C–C bond formation with the potential to effect chiral catalyst control.[6] Over the past two decades, our group and a number of other groups have described strategies to engage epoxides as electrophiles in Ni-catalyzed cross-coupling.[7] Weix and coworkers reported the first enantioselective cross-electrophile coupling with *meso*-epoxides using a chiral titanocene cocatalyst in conjunction with a racemic Ni catalyst (Figure 1B).[8] More recently, the Yamamoto group described the arylation of 3,4-epoxyalcohols using chiral bioxazoline (BiOx) ligands and Ni catalysis that furnishes cross-coupled products in excellent enantio- and diastereoselectivity (Figure 1B).[9] In this reaction, a pendant alcohol directing group is required on the epoxides for high stereoinduction. These important advances notwithstanding, the discovery and development of complementary methods, particularly to address the challenge of stereoconvergent cross-coupling with racemic terminal epoxides, is necessary to expand the scope and generality of this approach.

Recently, our group reported a photo-assisted reductive coupling (PARC) of racemic epoxides with aryl iodides via the merger of Ni-, Ti-, and photoredox catalysis.[7e] Mechanistic studies revealed that C–C bond formation with styrene oxides proceeds in a stereoablative manner, suggesting that the development of a stereoconvergent coupling of racemic epoxides with a chiral catalyst was mechanistically feasible. Herein, we describe a Ni/photoredox-catalyzed enantioselective cross-electrophile coupling of styrene oxides with aryl iodides using a chiral biimidazoline (BiIm) ligand (Figure 1C). This transformation allows facile access to enantioenriched 2,2-diarylalcohols, which could be readily derivatized to various chiral 1,1-diarylalkanes, a privileged motif in many natural products and bioactive molecules such as tolterodine and sertraline (Figure 1D).[10,11] Multivariate linear regression (MVLR) analysis with BiOx and BiIm ligands revealed that the electronic character of the ligands is the main contributor to enantioinduction differences between the ligands, as opposed to steric effects, which are typically responsible for stereoselectivity in asymmetric catalytic reactions. Further experimental and computational studies were conducted to interrogate this statistical model, ultimately providing support for a nonintuitive structure-selectivity relationship that may be of use in the design of other enantioselective Ni/photoredox cross-coupling reactions.

RESULTS AND DISCUSSIONS

Reaction Optimization.

Our optimization efforts focused on identifying an appropriate chiral ligand for the coupling of styrene oxide **1** and aryl iodide **2** using conditions derived from our prior work in racemic PARC of epoxides.[7e,12] Initial evaluation of common chiral amine-based bidentate ligands such as BOX, BiOx, PyrOx, QuinOx, PyBOX, and PHOX indicated that a variety of BiOx ligands–a high performing ligand class in our prior report on asymmetric reductive coupling of aziridines–offered good levels of enantioinduction (Figure S1, S2).[13] However, the desired cross-coupled product **3** was formed in low to moderate yield. Further optimization of other reaction components using **L1** as the ligand revealed that the titanocene cocatalyst required in our previously reported method is not needed in this transformation, while addition of catalytic $MgCl_2$ as a salt additive increases the reaction yield (Table 1, entry 1–3).[14]

Recently, chiral biimidazoline (BiIm) ligands[15] were shown to be effective in several enantioselective Ni-catalyzed reactions such as a benzylic C–H arylation and hydroarylation of vinylarenes.[16] Although the ligand class has not been applied to asymmetric cross-electrophile coupling, the structural similarity of BiIm and BiOx ligands, coupled with their additional site for derivatization, drew our interest. We prepared a small selection of known BiIm ligands (**L4**–**L6**) and evaluated them on our model reaction (entry 6–8). BiIm ligand **L6** furnished the desired product in 66% yield and 89% ee. Performing the reaction in a photoreactor further improved the yield to 70% with a slight increase in enantioselectivity to 91% ee (entry 9).[17] Control experiments indicated that Ni, ligand, photocatalyst, triethylamine (reductant), and light are required for the transformation (entry 10, 11a-d). We also found that the use of $Ir[dF(CF_3)ppy]_2(dtbbpy))PF_6$ in place of 1,2,3,5-tetrakis(carbazol-9-yl)-4,6-dicyanobenzene (4CzIPN) delivered the product in similar yield

and enantioselectivity, consistent with their similar excited state and ground state potentials (Figure S4).[18]

Substrate Scope.

With the optimized reaction conditions, we examined the reaction scope with respect to aryl iodides (Table 2). A wide range of *para*-substituted electron-rich and electron-deficient aryl iodides (**3**–**9**) underwent coupling in high enantioselectivity. In general, more electron-deficient aryl iodides afforded higher yields than electron-rich substrates. The reaction tolerates aryl iodides containing chlorine (**5**), pinacol boronic ester (**9**), and protic acetamide (**8**) groups, all of which may serve as functional group handles for further diversification. Nitrogen- and oxygen-containing heterocycles such as 2,3-dihydrobenzofuran (**14**), substituted pyridines (**15**–**17)**, and quinoline (**18**) are also well tolerated, demonstrating the potential for this protocol to be used in the synthesis of bioactive compounds. Additionally, while *meta*-substituted aryl iodides (**10**–**12**) are competent substrates under the reaction conditions, *ortho*-substituted aryl iodides delivered trace product presumably because steric hindrance of the electrophile deters productive chemistry.

Next, we proceeded to examine the scope of styrene oxides (Table 3). A wide range of *meta*- and *para*-substituted styrene oxides with electron-donating and electron-withdrawing functionalities (**19**–**25**) were compatible under the reaction conditions, generating products in moderate to good yield and ee's. Sterically hindered 2(*o*-tolyl)oxirane (**26**) underwent cross-coupling, albeit in lower yield and enantioselectivity. Nevertheless, the compatibility of *ortho*-substitution on the styrene oxide offers a strategic alternative to the limitation in the aryl iodide scope.

Mechanistic Investigations.

Previous Ni-catalyzed cross-coupling reactions of epoxides have been proposed to proceed by either (a) Ti-mediated radical ring-opening of the epoxide, (b) oxidative addition of Ni to the epoxide or (c) via the intermediacy of a halohydrin generated by nucleophilic ring-opening of epoxides with exogenous or *in situ*-generated salt additives.[7] Since a titanocene cocatalyst is not required for this enantioselective reaction, we sought to interrogate the impact of its omission on the reaction mechanism.

As evidence of the stereoconvergent nature of the reaction, subjecting both *R* and *S* enantiomers of styrene oxide **1** to the standard reaction conditions generated the enantioenriched product **3** in 63/75% yield and 91/91% ee respectively (Figure 2A).[19] To evaluate the alternative pathways for styrene oxide activation (b and c), we first performed competition experiments between 2-iodotoluene and styrene oxide with [dtbbpy]Ni^0(COD) (See SI). This experiment showed that aryl iodide undergoes exclusive oxidative addition to Ni(0), providing evidence against the former mechanism. As evidence in favor of the intermediacy of halohydrin, we subjected bromohydrin **27** to the standard reaction conditions in place of styrene oxide. Cross-coupled product **3** was obtained in enantioselectivity identical to that obtained in the model reaction with styrene oxide, albeit in lower yield (Figure 2B).[20] Furthermore, subjecting a catalytic amount (0.1 equiv) of

bromohydrin in the presence of 2-(*p*-tolyl)oxirane (0.9 equiv) yielded the corresponding products in 4% and 38% yield respectively, suggesting that halohydrin is likely an on-cycle intermediate (Figure S15).

Based on these studies, a Ni(0)/Ni(II)/Ni(III)/Ni(I) catalytic cycle involving a halohydrin intermediate is proposed (Figure 2C).[21] Oxidative addition of aryl iodide to Ni(0) **28** generates Ni(II) species **29**. At the same time, nucleophilic halide ring-opening of epoxide **1** by in-situ generated HX (X = Cl, Br, I from $MgCl_2$, $NiBr_2$·diglyme, and aryl iodide respectively) forms the halohydrin intermediate, which can undergo either single-electron transfer (SET) (with either **32** or 4CzIPN$^{-\bullet}$) or halogen atom abstraction or HAA (with **32**) to generate the corresponding secondary radical **30**. This radical can then be trapped by **29** to form Ni(III) species **31**, followed by reductive elimination to afford the cross-coupled product **3** and Ni(I) species **32**. The Ni(0) catalyst **28** can then be regenerated by reduction of **32** by 4CzIPN$^{-\bullet}$ ($PC/PC^{-\bullet}$ = −1.24 vs SCE, Ni(I)/Ni(0) = −1.17 vs SCE), which was generated via reductive quenching with Et_3N ($PC^*/PC^{-\bullet}$ = +1.43 vs SCE, $Et_3N^{+\bullet}/Et_3N$ = +0.93 vs SCE).[22]

Expansion of the Methodology.

The mechanistic experiment in Figure 2B suggested that iodide might not be necessary for the ring-opening step. This prompted us to consider using aryl bromides as electrophiles since there are generally more commercially available and less expensive than aryl iodides.[23] Indeed, subjecting aryl bromide **33** to the reaction conditions provided **3** in moderate yield and high ee (Figure 3A). Also, given the similarity of the mechanism between this work and our previously reported aziridine coupling, we envisioned that styrenyl aziridines could be used as coupling partners in place of styrene oxides. Employment of *N*-Ts aziridines **34** under the standard reaction conditions afforded the amine product **36** in 48% yield and 83% ee (Figure 3B). These results demonstrate the potential of this single reaction protocol to extend beyond styrene oxides and aryl iodides to access diverse chemical scaffolds bearing chiral 1,1-diaryl motifs.

Model Development.

In a prior report from our group on Ni-catalyzed enantioselective reductive coupling of aziridines, we performed MVLR analysis in collaboration with the Sigman lab using 17 BiOx ligands.[13] Since a 1,1-diarylmethane stereocenter is generated in both the epoxide and aziridine coupling reactions, we questioned whether similar effects might apply in the current study. We therefore sought to use statistical and computational tools to understand the key structural features of the BiIm ligands that influence enantioselectivity in the epoxide coupling, and through accompanying mechanistic studies, shed light on aspects of the reaction mechanism that are otherwise difficult to evaluate. To do so, we gathered enantioselectivity data from an extended scope of BiOx and BiIm ligands, generated computationally-derived features of the ligands, and performed MVLR analysis.[24]

A total of 20 BiOx and 9 BiIm ligands with diverse structure were evaluated under the reaction conditions shown in Figure 4A. We selected a number of parameters such as Sterimol values, molecular charges, and vibrational descriptors to describe the steric and

electronic properties of the ligands. Ground state structures were calculated by DFT at the M06–2X/def2TZVP[25] level of theory for three different coordination states of the ligands: the free ligand which was used in the aziridine study, a tetrahedral L*NiF_2 complex that serves as the most cost-effective surrogate to restrict the flexibility of the ligand, and a square planar L*Ni(*p*-tolyl)Cl complex which resembles possible on-cycle species in the catalytic cycle (Figure 4B).[26] Subsequently, features were acquired from these structures and were related to the enantioselectivity (expressed as $\Delta\Delta G^{\ddagger}$) in the MVLR analysis. By comparing models built from molecular descriptors extracted from different representations of the ligand, we sought to probe the structural complexity and associated computational cost of ligand representation sufficient to create a statistically robust descriptive model.

To assess predictive ability of a statistical model, leave-one-out and leave-*p*-out cross-validation are commonly used, especially in the context of small datasets. However, such methods may yield seemingly good performance metrics as an overwhelming majority of the dataset is used to train the model.[27] Instead, we employed a repeated stratified nested cross-validation method consisting of two cross-validation loops wherein the data was divided into train-validation/test splits and the inner loop is used to select regressor features (Figure 4B). This method has been shown to provide an almost unbiased estimate of true performance error in the identification of a robust predictive model.[28]

The best-performing model for each ligand representation was selected based on the number of times that model appeared to rank the highest (performance evaluated by RMSE) among the outer folds (Figure 4C). For L*Ni(*p*-tolyl)Cl complex, the final linear regression model (adj. $R^2 = 0.74$) consists of three independent parameters: $\boldsymbol{NBO_{N1}}$ (average NBO partial charge of the oxazoline/imidazoline nitrogen atoms), $\boldsymbol{NBO_{C4}}$ (average NBO partial charge of carbon atoms adjacent to the oxazoline/imidazoline ring), and ***Pol*** (polarizability). Similarly, the three-parameter models for the L*NiF_2 and free ligand representations exhibit at least two electronic parameters, highlighting the importance of ligand electronic character on the enantioselectivity. However, these models performed worse, giving adj. R^2 of 0.69 and 0.68 respectively. We also subjected each model to a 5×2 cross-validation test to compare model performance across different coordination states (See SI).[29] Overall, while more precise descriptors can be obtained from L*Ni(*p*-tolyl)Cl, our studies indicate that the free ligand descriptors are sufficient in constructing a descriptive model, thereby saving computational cost.

Since the models were acquired from scaled parameters, the magnitude and sign of the coefficients can give information about the effects of the features. For the L*Ni(*p*-tolyl)Cl model, enantioselectivity is largely governed by electronic effects, with more electron-donating ligands delivering higher levels of enantioselectivity (Figure 4C, middle). On the other hand, enantioselectivity is negatively correlated to polarizability.[30] To better visualize the features, we performed dimensionality reduction using principal component analysis (PCA) and plotted the data to show clusters based on their similarity (Figure 4C, right). We found that BiOx and BiIm ligands are separated by PC1 (46%) whose loadings are highly weighted toward electronic features, whereas PC2 (14%) splits BiOx into two clusters–Bn-BiOx and non-BnBiOx–based mostly on polarizability and steric features.

Eyring Analysis.

Finally, we sought to investigate how the electronic character of the ligands might influence enantioselectivity and experimentally validate the model. A seminal report by Jacobsen and coworkers demonstrated that more electron-donating Mn-salen catalysts led to higher enantioselectivity in an asymmetric epoxidation reaction as a result of a later, more product-like transition state structure in accordance with Hammond's postulate.[31] This prompted us to examine if a similar phenomenon was occurring in our system. An Eyring analysis was performed to determine the $\Delta\Delta H^{\ddagger}$ and $\Delta\Delta S^{\ddagger}$ between the major and minor diastereomeric transition states leading to both enantiomeric products. Energetic parameters were obtained on the model reaction using a systematic series of electronically distinct BiIm (**L6**–**L8**) and BiOx ligands (**L9**, **L1**) from 0 to 60°C. We found that the enthalpic component ($\Delta\Delta H^{\ddagger}$) of these reactions exhibits an upward trend with more electron-donating ligands, while the entropic contribution ($\Delta\Delta S^{\ddagger}$) does not show a clear trend (Figure 5A). In addition, the experimental $\Delta\Delta H^{\ddagger}$ is highly correlated with the calculated molecular charge feature $\boldsymbol{NBO_{N1}}$ ($R^2 = 0.96$), indicating that more electron-rich ligands within this study rely on enthalpic factors to afford high enantioselectivity and providing experimental validation for the statistical modeling (Figure 5B). The increasing magnitude of the differential enthalpy in the more electron-rich ligands is consistent with their accessing later transition state structures with more stabilizing (or destabilizing) interactions.

Computational Analysis.

Prior computational studies of related coupling reactions have suggested that either reductive elimination from Ni(III) or radical addition to tetrahedral Ni(II) is the enantiodetermining step.[32,33] In terms of substrate identity, this present work is more analogous to the system studied by Gutierrez, Kozlowski, and Molander where reductive elimination is enantiodetermining. In this case, a more electron-donating ligand would be expected to better stabilize Ni(III) leading to a less exergonic step and a later transition state structure according to the Hammond postulate. By contrast, the opposite trend might be expected if radical addition is stereodetermining as more electron-donating ligands could result in a less endergonic reaction to generate a stabilized Ni(III) species.

To interrogate these two possibilities, we performed computational analysis of the Ni catalytic cycle using **L6** as ligand, and bromobenzene and styrene oxide as substrates. Geometry optimization was performed at the UB3LYP functional and 6–31G(d) basis set. To compare energetics, we performed single point calculations of optimized structures using the UB3LYP-D3/6–311+G(d,p) level of theory with solvent correction (SMD solvation model in THF). Exhaustive conformational searches were performed for all intermediates to determine the lowest energy profile. Calculations showed that the singlet square planar Ni(II) generated from oxidative addition of aryl halide to Ni(0) can undergo intersystem crossing to form a triplet tetrahedral Ni(II) **B** that is 2.7 kcal/mol downhill in energy, similar to results from prior computational work by Gutierrez and Chu (Figure 6A).[33] The alkyl radical can then be intercepted by **B** to generate trigonal bipyramidal Ni(III) **C**, followed by C–C bond formation via reductive elimination to afford the coupled product and Ni(I) **D**. The generation of a square pyramidal Ni(III) **C'** proposed by Kozlowski and Molander

was also considered, but the relevant transition states were found to be energetically less favorable (see SI).

Calculations showed that the energy for the reductive elimination transition state **C-TS** is higher than the energy for the radical addition step **B-TS** (Figure 6B). This suggests that reductive elimination is the rate- and stereo-determining step, in agreement with our initial hypothesis. To gain insight into the origin of stereoselectivity, we calculated the minor diastereomeric reductive elimination transition state **C-TS-*R*,** which was found to be 1.7 kcal/mol uphill in energy compared to **C-TS-*S***. This energetic difference translates to 89% ee, in good agreement with the experimentally observed ee (91%). Non-covalent interaction (NCI) analysis revealed a repulsive interaction between the phenyl group on the radical and isopropyl group on the ligand in the transition state structure leading to the minor enantiomer of product. This result implies that the role of the chiral substituent in the optimal BiIm ligand is tied to a repulsive interaction in the diastereomeric transition state structure. In addition, the statistical modeling showed that the enantioselectivity difference between the ligands is mostly governed by electronic effects, leading to positional control of the transition states.[34] This effect would be hard to discern otherwise given the cost of performing transition state calculations for many different large ligand systems. Therefore, the statistical modeling and computational study have proven to be complementary in providing useful mechanistic insights to a complex catalytic system.

CONCLUSIONS

In conclusion, we have developed a Ni/photoredox catalyzed stereoconvergent coupling of styrene oxides with aryl iodides, allowing direct access to chiral 2,2-diarylalcohols in high enantioselectivity. Our study highlights the use of statistical modeling to elucidate a structure-selectivity relationship within a class of catalytic reactions that are otherwise mechanistically quite complex. These mechanistic findings offer insight into the design of improved chiral ligands in stereoconvergent Ni and Ni/photoredox cross-coupling. Future work in this area will focus on expanding this analysis to compare the classes of stereoconvergent coupling reactions that make use of nickel/biimidazoline and bioxazoline systems.

Supplementary Material

Refer to Web version on PubMed Central for supplementary material.

ACKNOWLEDGMENT

Financial support was provided by NIGMS R35 GM126986, F32 Ruth L. Kirschstein NRSA Fellowship under Award No. F32 EB027587-01 (T.J.S) and F32 Ruth L. Kirschstein NRSA Fellowship under Award No. F32 GM129910-01 (M.P.). The authors gratefully acknowledge Dr. Andrzej Żurański for assistance in ligand parameterization and modeling discussions.

Funding

The authors declare no competing financial interest.

REFERENCES

(1). Smith JG Synthetically Useful Reactions of Epoxides. Synthesis 1984, 1984, 629–656.

(2). For reviews on asymmetric epoxidation of olefins, see:(a)Johnson RA; Sharpless KB Asymmetric Oxidations and Related Reactions: Catalytic Asymmetric Epoxidation of Allylic Alcohols. In Catalytic Asymmetric Synthesis; John Wiley & Sons, Ltd, 2000; pp 229–280.(b)Katsuki T Asymmetric Oxidations and Related Reactions: Asymmetric Epoxidation of Unfunctionalized Olefins and Related Reactions. In Catalytic Asymmetric Synthesis; John Wiley & Sons, Ltd, 2000; pp 287–325.(c)Zhu Y; Wang Q; Cornwall RG; Shi Y Organocatalytic Asymmetric Epoxidation and Aziridination of Olefins and Their Synthetic Applications. Chem. Rev 2014, 114, 8199–8256. [PubMed: 24785198]

(3). Jacobsen EN Asymmetric Catalysis of Epoxide Ring-Opening Reactions. Acc. Chem. Res 2000, 33, 421–431. [PubMed: 10891060]

(4). For reviews on asymmetric ring-opening of epoxides, see:(a)Lidskog A; Li Y; Wärnmark K Asymmetric Ring-Opening of Epoxides Catalyzed by Metal–Salen Complexes. Catalysts 2020, 10, 705.(b)Pastor I; Yus M Asymmetric Ring Opening of Epoxides. Curr. Org. Chem 2005, 9, 1–29.

(5). Oguni N; Miyagi Y; Itoh K Highly Enantioselective Arylation of Symmetrical Epoxides with Phenyllithium Promoted by Chiral Schiff Bases and Salens. Tet. Lett 1998, 39, 9023–9026.

(6). Huang C-Y; Doyle AG The Chemistry of Transition Metals with Three-Membered Ring Heterocycles. Chem. Rev 2014, 114, 8153–8198. [PubMed: 24869559]

(7). (a)Molinaro C; Jamison TF Nickel-Catalyzed Reductive Coupling of Alkynes and Epoxides. J. Am. Chem. Soc 2003, 125, 8076–8077. [PubMed: 12837057] (b)Molinaro C; Jamison TF Catalytic Reductive Coupling of Epoxides and Aldehydes: Epoxide-Ring Opening Precedes Carbonyl Reduction. Angew. Chem. Int. Ed 2005, 44, 129–132.(c)Nielsen DK; Doyle AG Nickel-Catalyzed Cross-Coupling of Styrenyl Epoxides with Boronic Acids. Angew. Chem. Int. Ed 2011, 50, 6056–6059.(d)Zhao Y; Weix DJ Nickel-Catalyzed Regiodivergent Opening of Epoxides with Aryl Halides: Co-Catalysis Controls Regioselectivity. J. Am. Chem. Soc 2014, 136, 48–51. [PubMed: 24341892] (e)Parasram M; Shields BJ; Ahmad O; Knauber T; Doyle AG Regioselective Cross-Electrophile Coupling of Epoxides and (Hetero)Aryl Iodides via Ni/Ti/Photoredox Catalysis. ACS Catal 2020, 10, 5821–5827. [PubMed: 32747870] (f)Lin Z; Lan Y; Wang C Ligand-Free Nickel-Catalyzed Reductive Allylic Defluorinative Cross-Coupling of α-Trifluoromethyl Alkenes with Epoxides. Synlett. 2020, 31, A–D.(g)Lu X-Y; Jiang R-C; Li J-M; Liu C-C; Wang Q-Q; Zhou H-P Synthesis of Gem-Difluoroalkenes via Nickel-Catalyzed Allylic Defluorinative Reductive Cross-Coupling of Trifluoromethyl Alkenes with Epoxides. Org. Biomol. Chem 2020, 18, 3674–3678. [PubMed: 32377647] (h)Potrzasaj A; Musiejuk M; Chaładaj W; Giedyk M; Gryko D Cobalt Catalyst Determines Regioselectivity in Ring Opening of Epoxides with Aryl Halides. J. Am. Chem. Soc 2021. 143, 9368–9376. [PubMed: 34081860]

(8). Zhao Y; Weix DJ Enantioselective Cross-Coupling of Meso-Epoxides with Aryl Halides. J. Am. Chem. Soc 2015, 137, 3237–3240. [PubMed: 25716775]

(9). Banerjee A; Yamamoto H Nickel Catalyzed Regio-, Diastereo-, and Enantioselective Cross-Coupling of 3,4-Epoxyalcohol with Aryl Iodides. Org. Lett 2017, 19, 4363–4366. [PubMed: 28753019]

(10). (a)Hills CJ; Winter SA; Balfour JA Tolterodine. Drugs 1998, 55, 813–820. [PubMed: 9617596] (b)McRae AL; Brady KT Review of Sertraline and its Clinical Applications in Psychiatric Disorders. Expert Opin. Pharmacother 2001, 2, 883–892. [PubMed: 11336629] (c)Asp V; Cantillana T; Bergman A; Brandt I Chiral Effects in Adrenocorticolytic Action of *o,p'*-DDD (Mitotane) in Human Adrenal Cells. Xenobiotica, 2010, 40, 177–183. [PubMed: 20044879] For a review on chiral 1,1-diaryl compounds, see:(d)Ameen D; Snape TJ Chiral 1,1-Diaryl Compounds as Important Pharmacophores. MedChemComm 2013, 4, 893–907.

(11). To our knowledge, there is no example of transition-metal catalyzed stereospecific arylation of enantioenriched styrene oxides. Moreover, reactions using organolithium reagents are known but the linear product is favored, see:(a)Ertürk E; Tezeren MA; Atalar T; Tilki T Regioselective Ring-Opening of Epoxides with Ortho-Lithioanisoles Catalyzed by $BF_3{\cdot}OEt_2$. Tetrahedron, 2012, 68, 6463–6471.(b)Dilek Ö; Tezeren MA; Tilki T; Ertürk E Chiral 2-(2-Hydroxyaryl)Alcohols

(HAROLs) with a 1,4-Diol Scaffold as a New Family of Ligands and Organocatalysts. Tetrahedron, 2018, 74, 268–286;The scope of Friedel-Craft alkylation with styrene oxides is also limited to electron-rich arenes, see:(c)Li G-X; Qu J Friedel–Crafts Alkylation of Arenes with Epoxides Promoted by Fluorinated Alcohols or Water. Chem. Commun 2010, 46, 2653–2655. (d)Bertolini F; Crotti P; Macchia F; Pineschi MA New Regio- and Stereoselective Intermolecular Friedel–Crafts Alkylation of Phenolic Substrates with Aryl Epoxides. Tet. Lett 2006, 47, 61–64. (e)Kim Y; Choi YS; Hong SK; Park YS Friedel–Crafts Alkylation with α-Bromoarylacetates for the Preparation of Enantioenriched 2, 2-Diarylethanols. Org. Biomol. Chem 2019, 17, 4554–4563. [PubMed: 30994667] Alternatively, similar products can be generated by cross-electrophile coupling of aryl iodides and benzylic chlorides. However, protection of the alcohol group is required.(f)Poremba KE; Kadunce NT; Suzuki N; Cherney AH; Reisman SE Nickel-Catalyzed Asymmetric Reductive Cross-Coupling to Access 1,1-Diarylalkanes. J. Am. Chem. Soc 2017, 139, 5684–5687. [PubMed: 28406620]

(12). Initial reaction conditions: $NiBr_2$·diglyme (10 mol%), ligand (15 mol%), 4CzIPN (5 mol%), Cp_2TiCl_2 (25 mol% or 0 mol%), Et_3N (5 equiv), MgCl2 (25 mol%), 2-(4-fluorophenyl)oxirane (1 equiv, 0.05 mmol), 4-iodobiphenyl (3 equiv), MeCN (0.033 M). See SI for more details.[2223]

(13). (a)Woods BP; Orlandi M; Huang C-Y; Sigman MS; Doyle AG Nickel-Catalyzed Enantioselective Reductive Cross-Coupling of Styrenyl Aziridines. J. Am. Chem. Soc 2017, 139, 5688–5691. [PubMed: 28406622] (b)Woods BP; Orlandi M; Huang C-Y; Sigman MS; Doyle AG Correction to “Nickel-Catalyzed Enantioselective Reductive Cross-Coupling of Styrenyl Aziridines.” J. Am. Chem. Soc 2018, 140, 7744–7745. [PubMed: 29889505]

(14). $MgCl_2$ is used as an additive to activate epoxides toward ring-opening.Magre M; Paffenholz E; Maity B; Cavallo L; Rueping M Regiodivergent Hydroborative Ring Opening of Epoxides via Selective C–O Bond Activation. J. Am. Chem. Soc 2020, 142, 14286–14294. [PubMed: 32658463]

(15). (a)Boland NA; Casey M; Hynes SJ; Matthews JW; Müller-Bunz H; Wilkes P Preparation of Enantiopure Biimidazoline Ligands and Their Use in Asymmetric Catalysis. Org. Biomol. Chem 2004, 2, 1995–2002. [PubMed: 15254626] (b)Hao X-Q; Dong Y-N; Gao B; Li K; Zhao X-M; Xu Y; Song M-P Biimidazoline Ligands for Palladium-Catalyzed Asymmetric Allylic Alkylation. Tetrahedron: Asymmetry 2015, 26, 1360–1368.(c)Li J; Yu B; Lu Z Chiral Imidazoline Ligands and Their Applications in Metal-Catalyzed Asymmetric Synthesis. Chin. J. Chem 2021, 39, 488–514.

(16). (a)Cheng X; Lu H; Lu Z Enantioselective Benzylic C–H Arylation via Photoredox and Nickel Dual Catalysis. Nat. Commun 2019, 10, 3549. [PubMed: 31391466] (b)He Y; Liu C; Yu L; Zhu S Enantio- and Regioselective NiH-Catalyzed Reductive Hydroarylation of Vinylarenes with Aryl Iodides. Angew. Chem. Int. Ed 2020, 59, 21530–21534.(c)Cuesta-Galisteo S; Schörgenhumer J; Wei X; Merino E; Nevado C Nickel-Catalyzed Asymmetric Synthesis of α-Arylbenzamides. Angew. Chem. Int. Ed 2021, 60, 1605–1609.(d)He Y; Song H; Chen J; Zhu S NiH-Catalyzed Asymmetric Hydroarylation of *N*-Acyl Enamines to Chiral Benzylamines. Nat. Commun 2021, 12, 638. [PubMed: 33504793] (e)Zhou P; Li X; Wang D; Xu T Dual Nickel- and Photoredox-Catalyzed Reductive Cross-Coupling to Access Chiral Trifluoromethylated Alkanes. Org. Lett 2021, 23, 4683–4687. [PubMed: 34077223]

(17). Penn PhD photoreactor has been shown to provide cooling to maintain a reaction temperature at 24 to 25 °C.Le C; Wismer MK; Shi Z-C; Zhang R; Conway DV; Li G; Vachal P; Davies IW; MacMillan DWC A General Small-Scale Reactor To Enable Standardization and Acceleration of Photocatalytic Reactions. ACS Cent. Sci 2017, 3, 647–653. [PubMed: 28691077]

(18). (a)Lowry MS; Goldsmith JI; Slinker JD; Rohl R; Pascal RA; Malliaras GG; Bernhard S Single-Layer Electroluminescent Devices and Photoinduced Hydrogen Production from an Ionic Iridium(III) Complex. Chem. Mater 2005, 17, 5712.(b)Luo J; Zhang J Donor-Acceptor Fluorophores for Visible-Light-Promoted Organic Synthesis: Photoredox/Ni Dual Catalytic $C(sp^3)$-$C(sp^2)$ Cross-Coupling. ACS Catal 2016, 6, 873.

(19). Replacing **(*S*,*S*)-L6** with the opposite enantiomer **(*R*,*R*)-L6** under otherwise identical reaction conditions afforded the enantioenriched product **13** in comparable yield and opposite enantioselectivity of similar magnitude. See SI.**(*S*,*S*)-L6(*R*,*R*)-L613**

(20). Subjecting iodohydrin to the reaction condition resulted in no product formation. We attribute this lack of reactivity to catalyst deactivation by iodide. Consistent with this proposal, we found that

adding tetrabutylammonium iodide (1 equiv) as an additive in the model reaction significantly reduces the yield. See SI for more details.

(21). (a)Steiman TJ; Liu J; Mengiste A; Doyle AG Synthesis of β-Phenethylamines via Ni/Photoredox Cross-Electrophile Coupling of Aliphatic Aziridines and Aryl Iodides. J. Am. Chem. Soc 2020, 142, 7598–7605. [PubMed: 32250602] (b)Arp FO; Fu GC Catalytic Enantioselective Negishi Reactions of Racemic Secondary Benzylic Halides. J. Am. Chem. Soc 2005, 127, 10482–10483. [PubMed: 16045323] For reviews on Ni-catalyzed stereoconvergent coupling with alkyl electrophiles, see:(c)Poremba KE; Dibrell SE; Reisman SE Nickel-Catalyzed Enantioselective Reductive Cross-Coupling Reactions. ACS Catal 2020, 10, 8237–8246, [PubMed: 32905517] (d)Lipp A; Badir SO; Molander GA Stereoinduction in Metallaphotoredox Catalysis. Angew. Chem. Int. Ed 2021, 60, 1714–1726.

(22). (a)Shields BJ; Doyle AG Direct C(sp^3)–H Cross Coupling Enabled by Catalytic Generation of Chlorine Radicals. J. Am. Chem. Soc 2016, 138, 12719–12722. [PubMed: 27653738] (b)Shang T-Y; Lu L-H; Cao Z; Liu Y; He W-M; Yu B Recent Advances of 1,2,3,5-tetrakis(carbazole-9-ul)-4,6-dicyanobenzene (4CzIPN) in Photocatalytic Transformations. Chem. Commun 2019, 55, 5408–5419.(c)Speckmeier E; Fischer TG; Zeitler K A Toolbox Approach to Construct Broadly Applicable Metal-Free Catalysts for Photoredox Chemistry: Deliberate Tuning of Redox Potentials and Importance of Halogen in Donor-Acceptor Cyanoarenes. J. Am. Chem. Soc 2018, 140, 15353–15365. [PubMed: 30277767]

(23). Commercial availability of aryl halides: ArI (200,946 based on substructure search of phenyl iodide), ArBr (707,280 based on substructure search of phenyl bromide). Source: eMolecules database, accessed July 25, 2021 using Elsevier Reaxys.

(24). Sigman MS; Harper KC; Bess EN; Milo A The Development of Multidimentsional Analysis Tools for Asymmetric Catalysis and Beyond. Acc. Chem. Res 2016, 49, 1292–1301. [PubMed: 27220055]

(25). This functional/basis set combination, previously used in our prior work on asymmetric aziridine coupling (ref. 12), was used for both free ligands and nickel complexes to ensure direct comparison among the different ligand representations. Models acquired from free ligand and L*Ni(*p*-tolyl)Cl using M06/def2TZVP level of theory and their corresponding 5×2 cross-validation tests provide comparable results. See SI for more details.

(26). Yin H; Fu GC Mechanistic Investigation of Enantioconvergent Kumada Reactions of Racemic α-Bromoketones Catalyzed by a Nickel/Bis(Oxazoline) Complex. J. Am. Chem. Soc 2019, 141, 15433–15440. [PubMed: 31502449]

(27). Hastie T; Tibshirani R; Friedman J The Elements of Statistical Learning: Data Mining, Inference, and Prediction.; Springer US: Boston, MA, 2009.

(28). Varma S; Simon R Bias in Error Estimation When Using Cross-Validation for Model Selection. BMC Bioinformatics 2006, 7, 91. [PubMed: 16504092]

(29). Dietterich TG Approximate Statistical Tests for Comparing Supervised Classification Learning Algorithms. Neural Computation 1998, 10, 1895–1923. [PubMed: 9744903]

(30). This observation can be attributed to the strong correlation between DFT-derived isotropic polarizability and the carbon count on the ligands, where the effect is more pronounced within BiOx ligands. See SI.

(31). (a)Jacobsen EN; Zhang W; Güler ML Electronic Tuning of Asymmetric Catalysts. J. Am. Chem. Soc 1991, 113, 6703–6704.(b)Palucki M; Finney NS; Pospisil PJ; Güler ML; Ishida T; Jacobsen EN The Mechanistic Basis for Electronic Effects on Enantioselectivity in the (Salen)Mn(III)-Catalyzed Epoxidation Reaction. J. Am. Chem. Soc 1998, 120, 948–954.

(32). (a)Gutierrez O; Tellis JC; Primer DN; Molander GA; Kozlowski MC Nickel-Catalyzed Cross-Coupling of Photoredox-Generated Radicals: Uncovering a General Manifold for Stereoconvergence in Nickel-Catalyzed Cross-Couplings. J. Am. Chem. Soc 2015, 137, 4896–4899. [PubMed: 25836634] (b)Yuan M; Song Z; Badir SO; Molander GA; Gutierrez O On the Nature of C(sp^3)–C(sp^2) Bond Formation in Nickel-Catalyzed Tertiary Radical Cross-Couplings: A Case Study of Ni/Photoredox Catalytic Cross-Coupling of Alkyl Radicals and Aryl Halides. J. Am. Chem. Soc 2020, 142, 7225–7234. [PubMed: 32195579]

(33). Guo L; Yuan M; Zhang Y; Wang F; Zhu S; Gutierrez O; Chu L General Method for Enantioselective Three-Component Carboarylation of Alkenes Enabled by Visible-Light Dual Photoredox/Nickel Catalysis. J. Am. Chem. Soc 2020, 142, 20390–20399.

(34). We have attempted to investigate this effect using DFT; however, we could not locate the reductive elimination transition state structure for **L8**. See SI for more details.**L8**

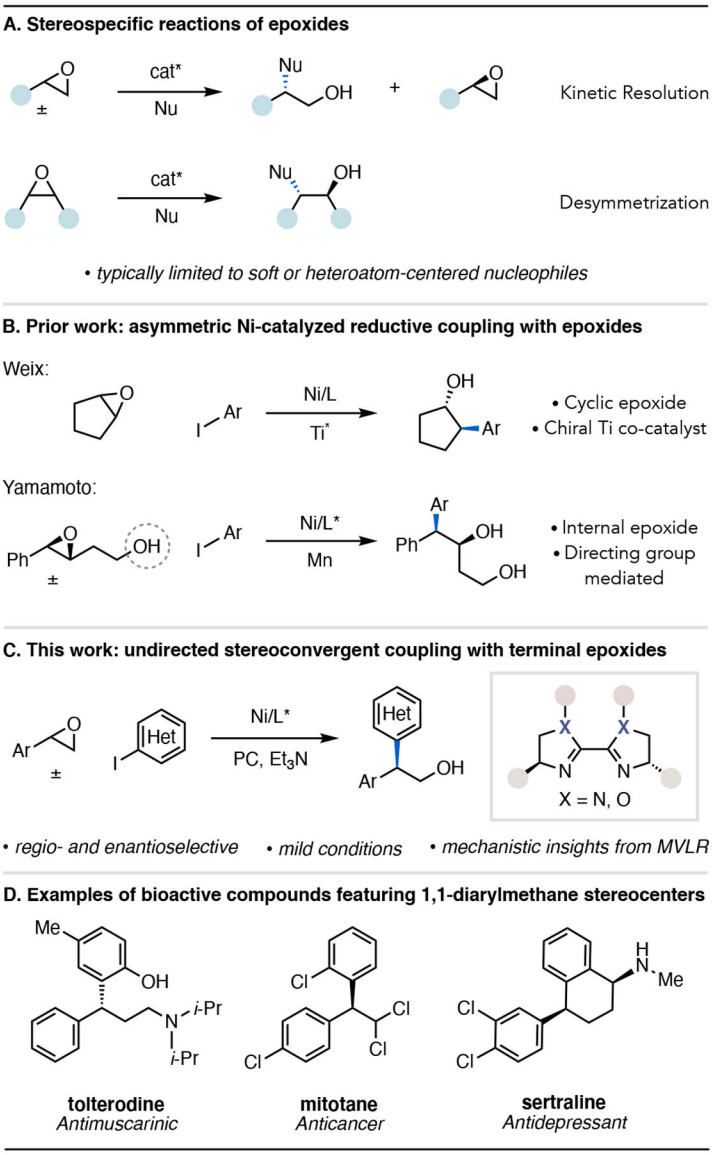

Figure 1.
Strategies for asymmetric synthesis with epoxides.

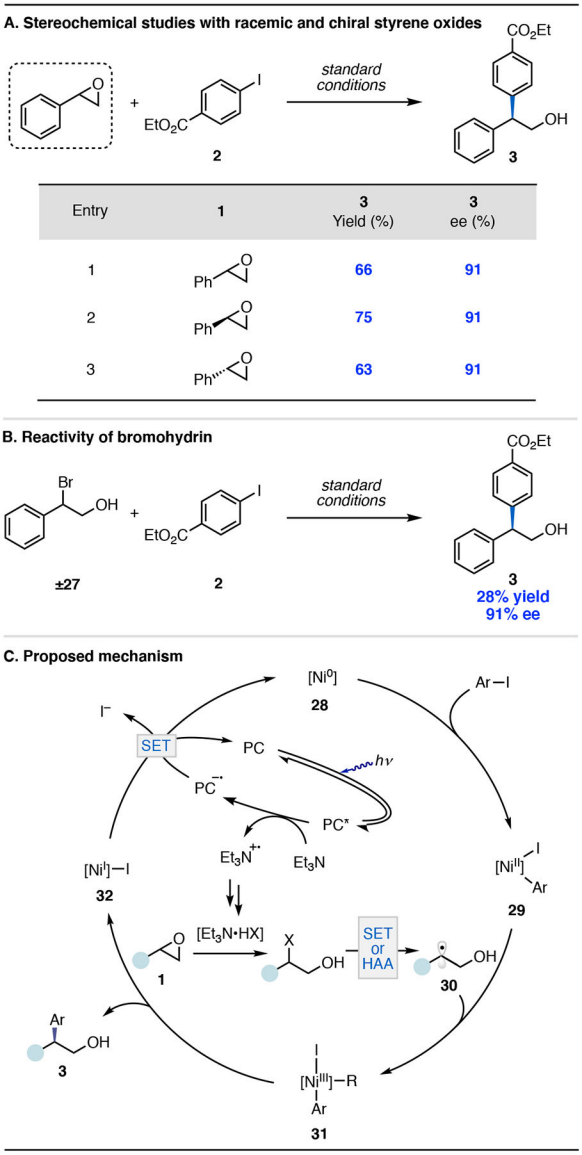

Figure 2.
Mechanistic Studies.

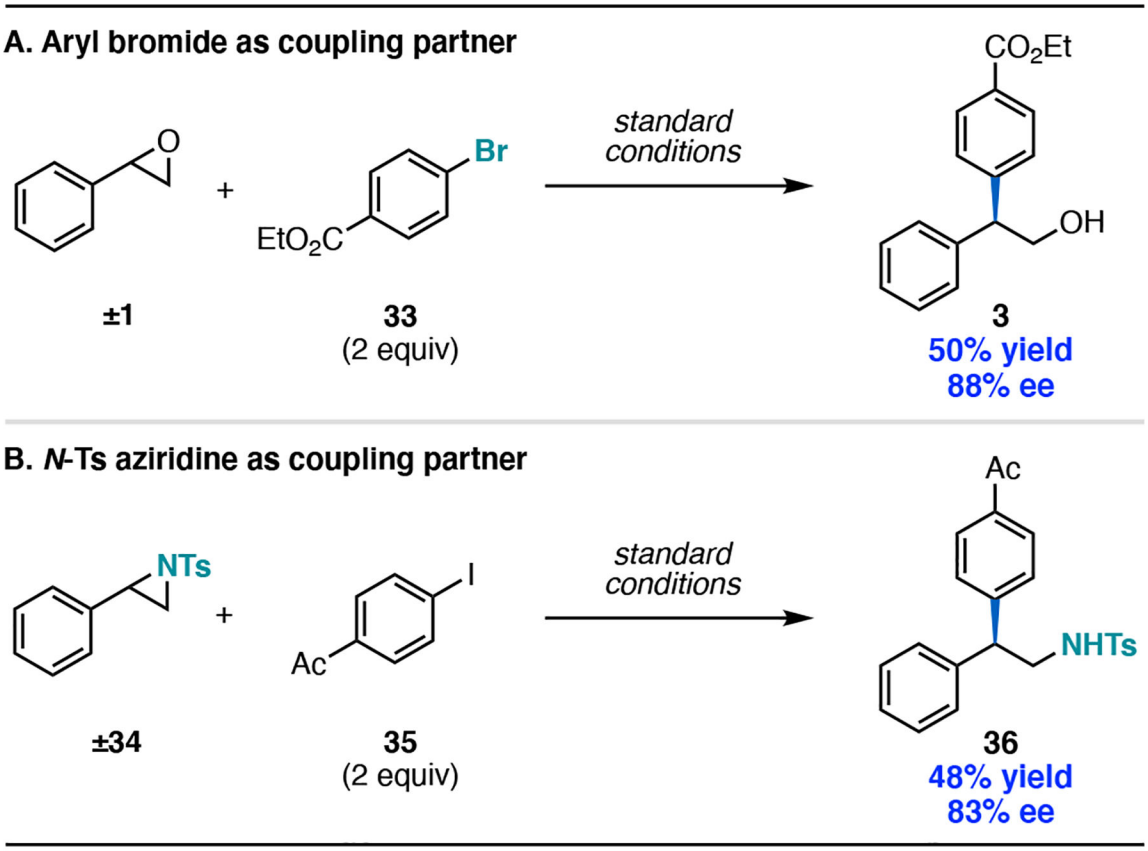

Figure 3.
Expansion of scope.

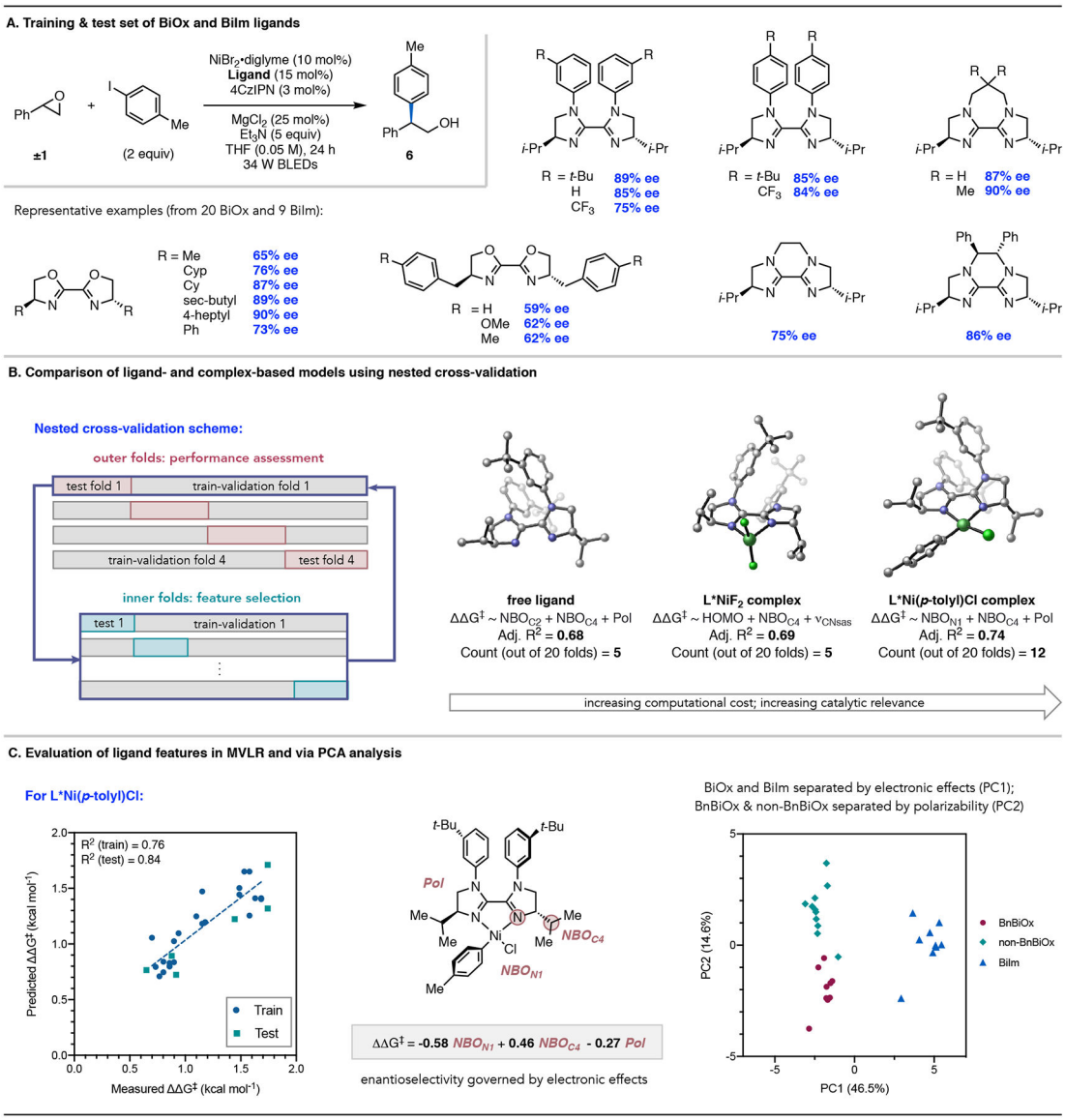

Figure 4.
Computational and statistical analysis.

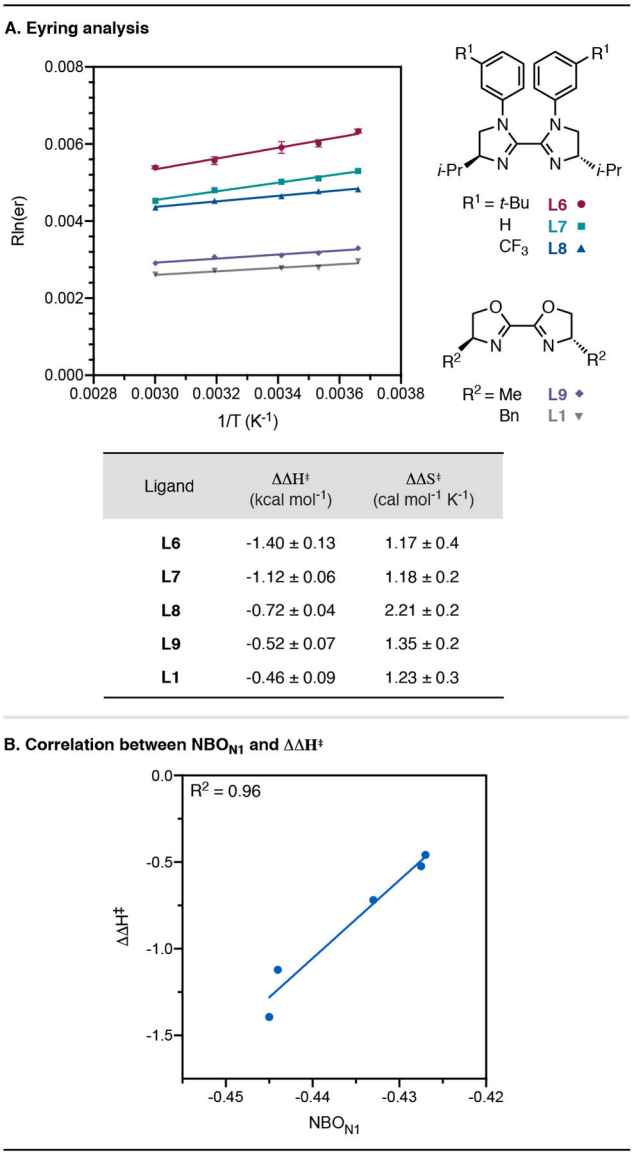

Ligand	ΔΔH‡ (kcal mol-1)	ΔΔS‡ (cal mol-1 K-1)
L6	-1.40 ± 0.13	1.17 ± 0.4
L7	-1.12 ± 0.06	1.18 ± 0.2
L8	-0.72 ± 0.04	2.21 ± 0.2
L9	-0.52 ± 0.07	1.35 ± 0.2
L1	-0.46 ± 0.09	1.23 ± 0.3

Figure 5.
Eyring Analysis.

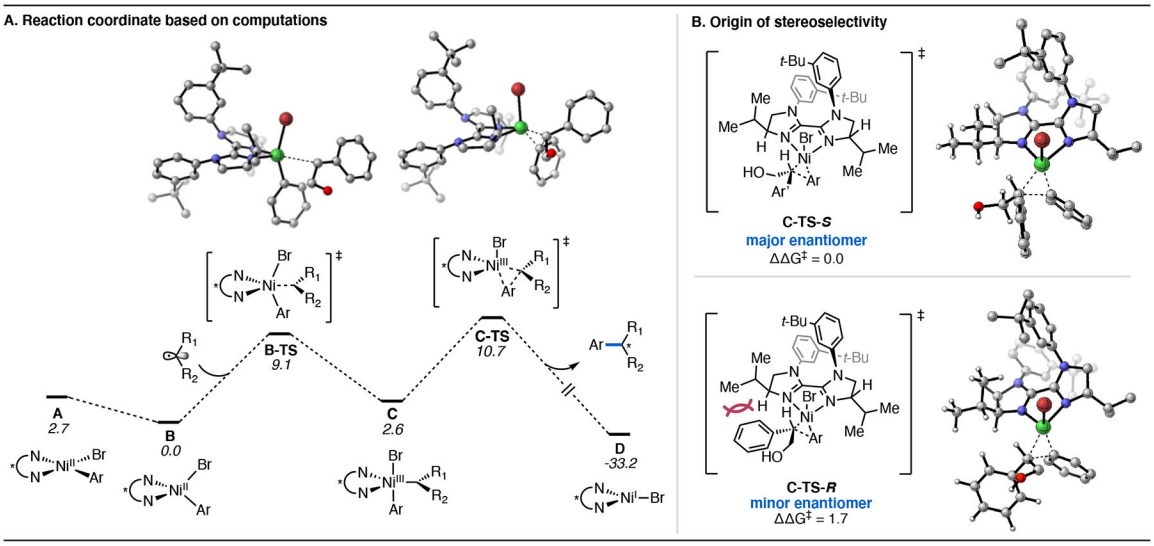

Figure 6.

Computational analysis. [a]All free energies are in kcal/mol, and were calculated at the UB3LYP-D3/6–311+G(d,p)/SMD(THF) level of theory.

Table 1.

Reaction optimization.

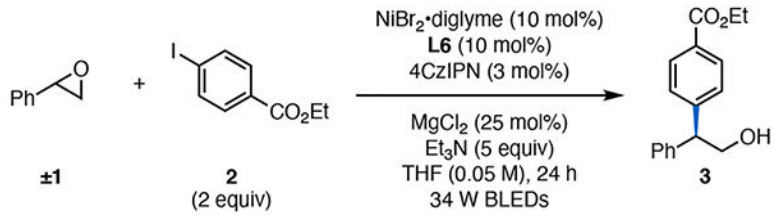

Entry	Deviation from standard conditions	3 Yield (%)[a]	3 ee (%)[b]
1	**L1**, no $MgCl_2$ and with Cp_2TiCl_2 (25 mol%)	30[c]	58
2	**L1**, no $MgCl_2$	41[c]	56
3	**L1**	63	59
4	**L2**	12	81
5	**L3**	30	92
6	**L4**	24	86
7	**L5**	45	89
8	none	66	89
9	**Photoreactor** [d]	**70**	**91**
10	no **L6**	3	0
11a-d	no Ni, 4CzIPN, Et_3N, or light	0	n.d.

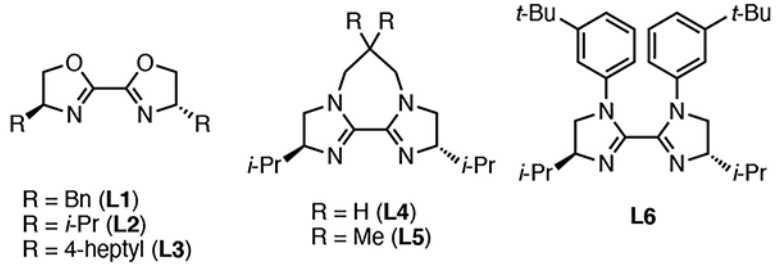

[a]Determined by GC (0.05 mmol).

[b]Determined by chiral HPLC.

[c]Determined by NMR.

[d]Penn PhD photoreactor (450 nm) on 0.5 mmol scale.

Table 2.

Scope of aryl iodide.

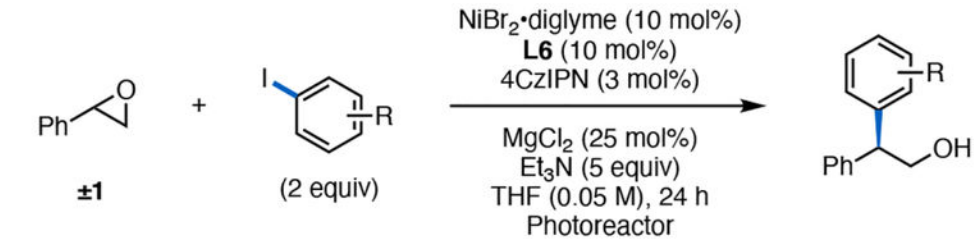

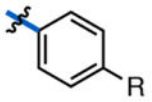	3, R = CO_2Et 4, R = CF_3 5, R = Cl 6, R = Me 7, R = OMe 8, R = NHAc 9, R = BPin	65% yield, 90% ee 67% yield, 88% ee 64% yield, 87% ee 45% yield, 90% ee 29% yield, 90% ee 36% yield, 90% ee 50% yield, 93% ee
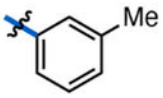	**10** 42% yield 90% ee	
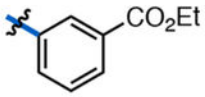	**11** 52% yield 87% ee	
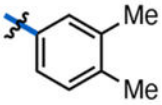	**12** 50% yield 90% ee	
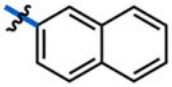	**13** 54% yield 91% ee	
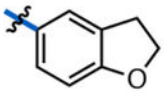	**14** 30% yield 91% ee	
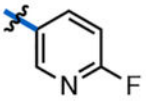	**15** 49% yield 76% ee	
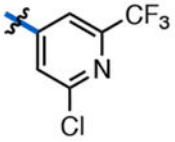	**16** 58% yield 78% ee	
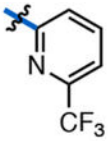	**17** 59% yield 55% ee	
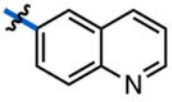	**18** 50% yield 90% ee	
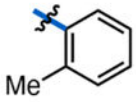	<5% yield	

[a]Yield and ee are average of two runs (0.5 mmol).

Table 3.

Scope of epoxides.

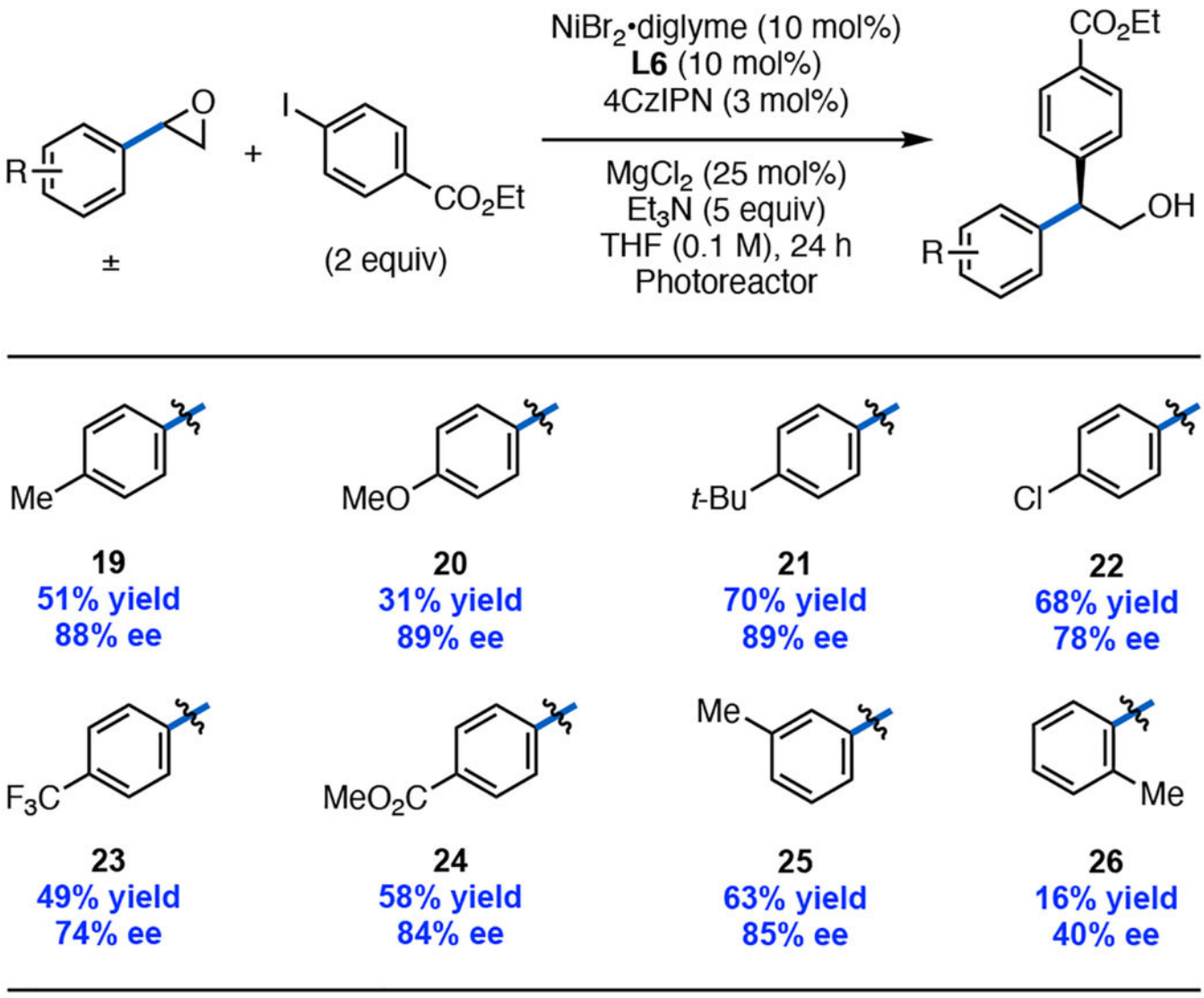

[a]Yield and ee are average of two runs (0.5 mmol).